Electronic Supplementary Material (ESI) for Journal of Materials Chemistry A.

Supporting Information

Endowing rGO Superior Cations/Anions Co-purification and Visible Photocatalysis Performances by In-Situ Deposition of Silver Compound

Ye Xiong,[a] Chao Wang,[a] Hanwei Wang,[a] Chunde Jin,[a] Qingfeng Sun[*a] and Xijin Xu[*b]

a. School of Engineering, Zhejiang A & F University, Hangzhou, Zhejiang Province, 311300, PR China

b. Key Laboratory of Wood Science and Technology, Zhejiang Province, 311300, PR China.

***Corresponding author:** Qingfeng Sun and Xijin Xu

E-mail: qfsun@zafu.edu.cn, sps_xuxj@ujn.edu.cn

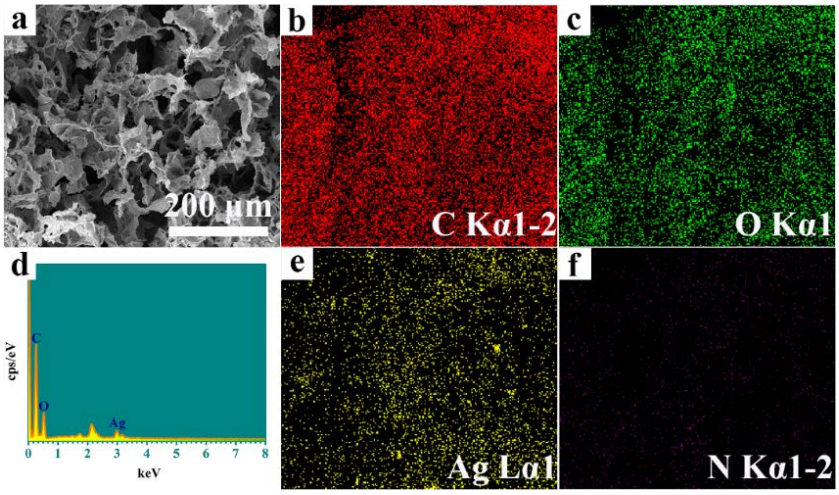

Figure S1. (a) SEM image of Ag_2O/rGO, **(d)** EDS spectrum of Ag_2O/rGO aerogel and the corresponding elemental mapping images: **(b)** C; **(c)** O; **(e)** Ag; **(f)** N.

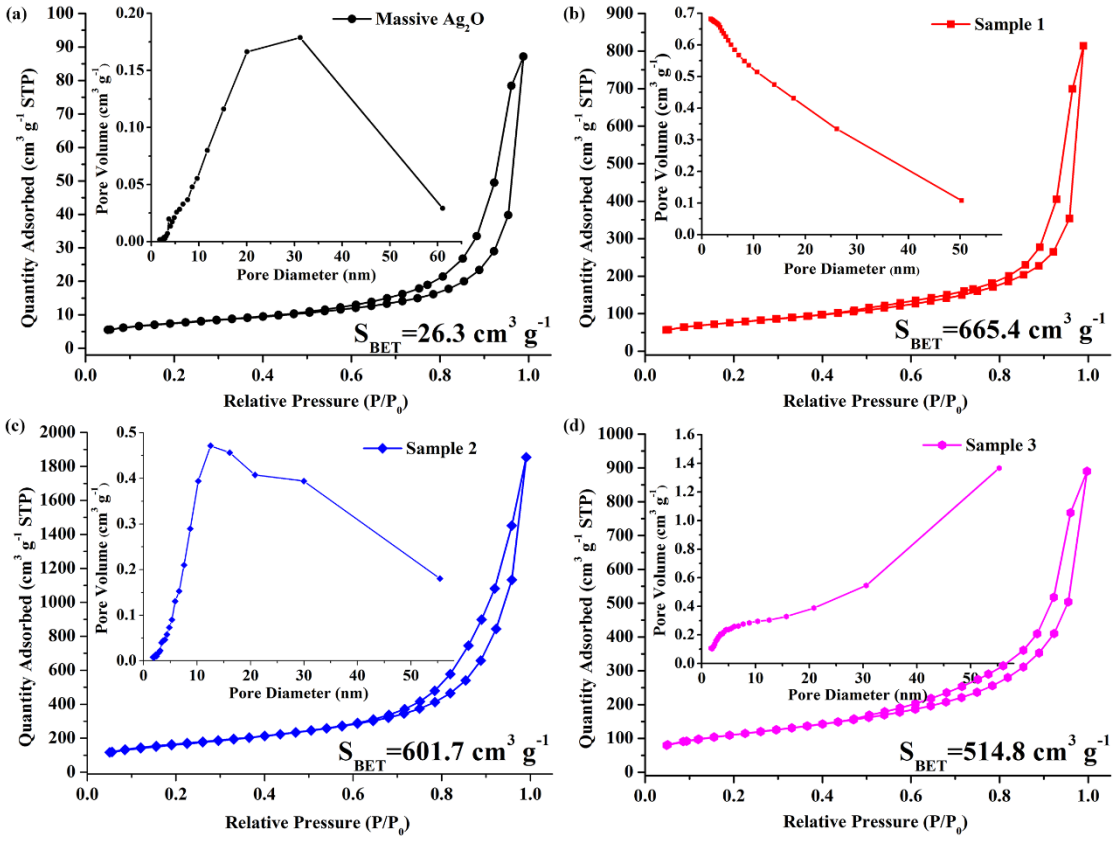

Figure S2. N_2 adsorption-desorption isotherms of the massive Ag_2O and sample A1-A3, respectively.

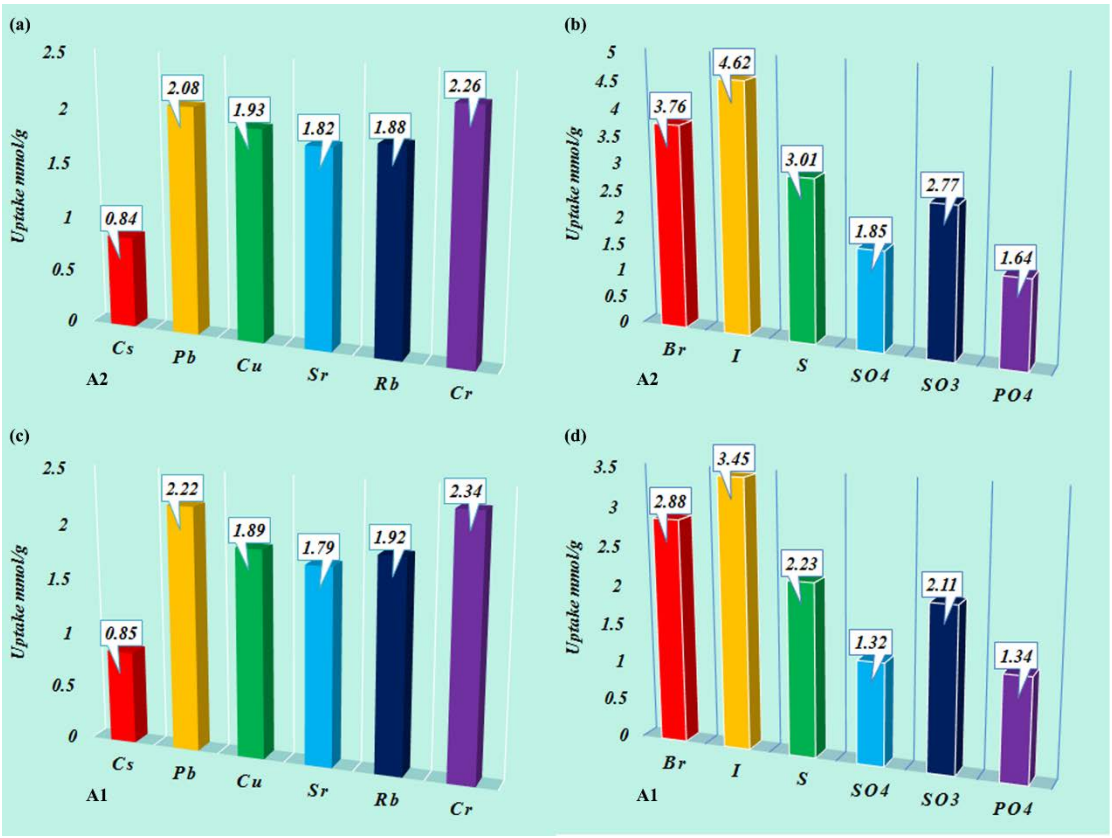

Figure S3. (a) and **(c)** Cationic adsorption performance of samples A2 and A1, respectively. **(b)** and **(d)** Anionic adsorption performance of samples A2 and A1, respectively.

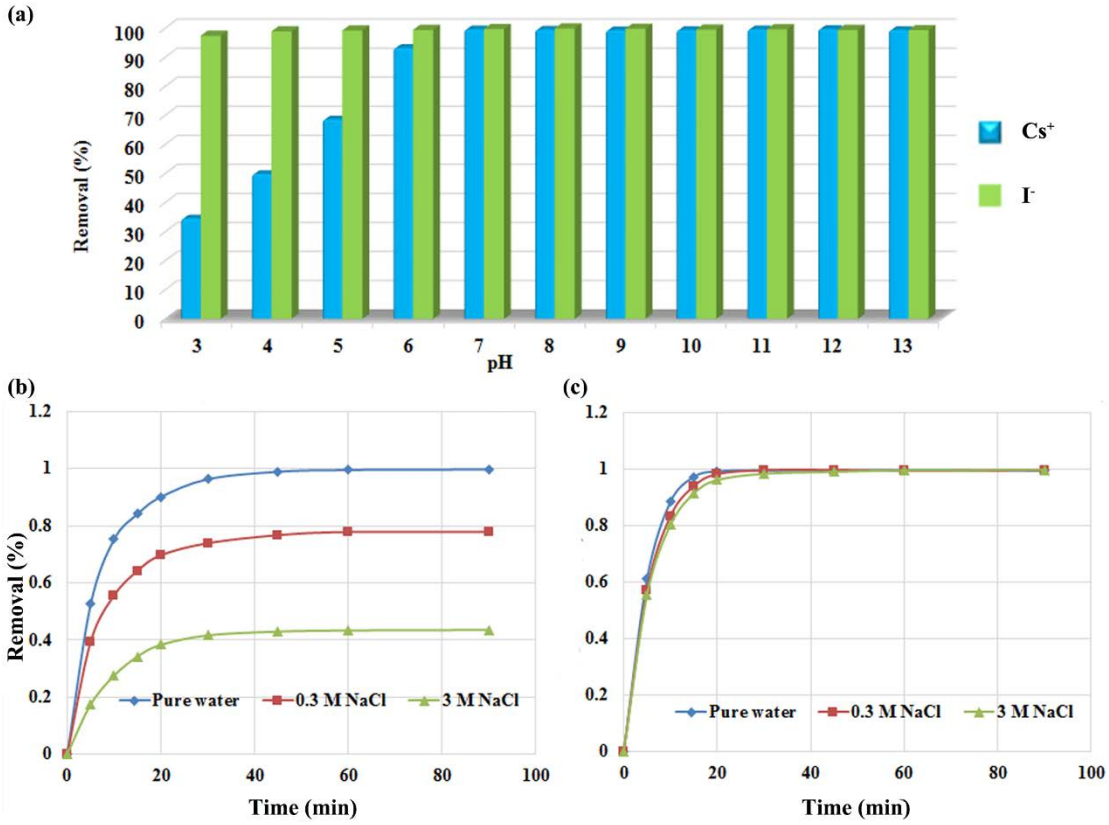

Figure S4. (a) Co-purification performances of Cationic Cs^+ and anionic I^- by sample 3 in the pH range of 3~11. **(b)** and **(c)** Competitive adsorption of Cationic Cs^+ and anionic I^- on Ag_2O/rGO aerogels.

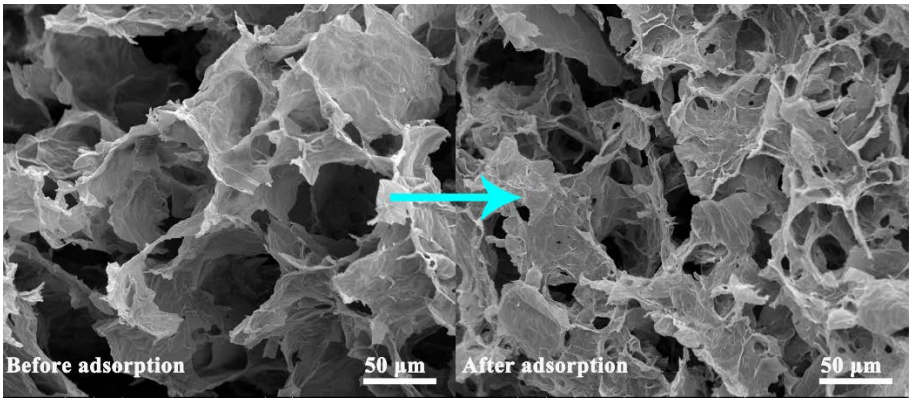

Figure S5. Morphology of the Ag_2O/rGO aerogel before and after adsorption.

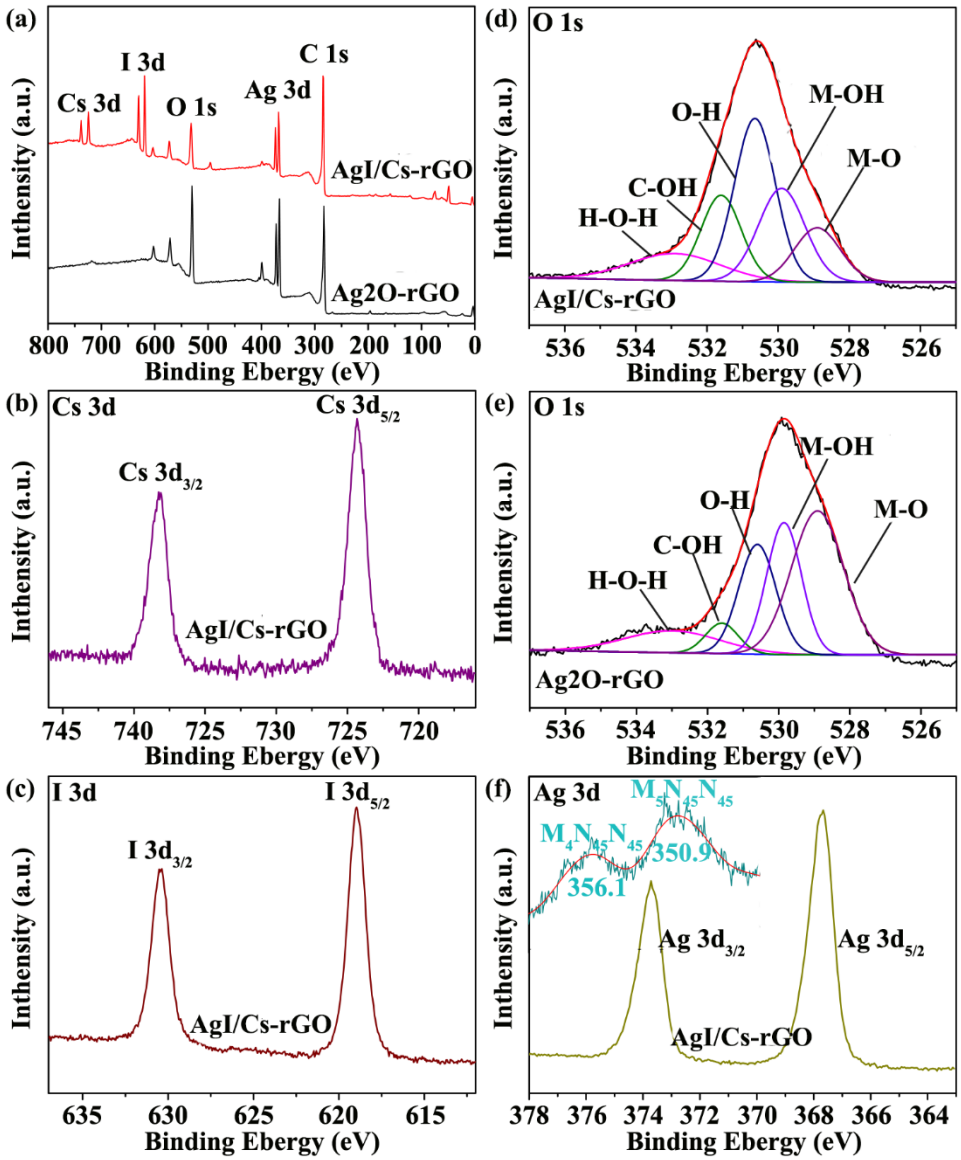

Figure S6. XPS spectra of the Ag_2O/rGO hybrid aerogel before and after co-capturing Cs^+ and I^-: **(a)** survey spectrum; **(b)** Cs 3d; **(c)** I 3d; **(d)** and **(e)**O 1s; **(f)** Ag 3d, inside: Ag MNN.

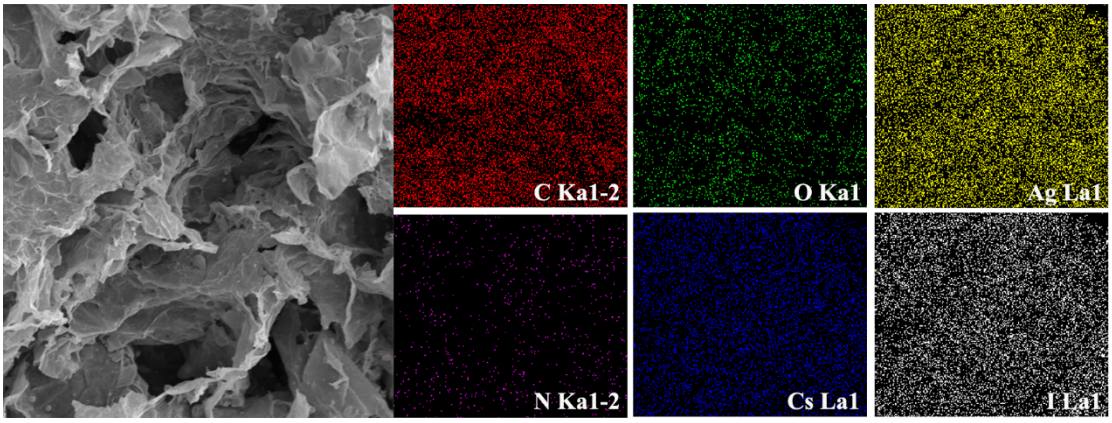

Figure S7. Energy mapping images of Ag_2O/rGO aerogels after treated with CsI solution for 48 h.

Element	Weight percentage (%)	Atomic percent (%)
C K	11.16	46.55
O K	5.89	18.43
Ag L	34.65	16.09
I L	40.76	16.09
Cs L	7.54	2.84
Total	100.00	100.00

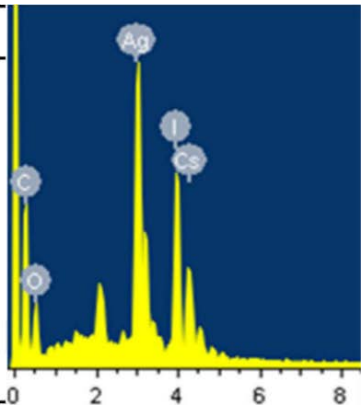

Figure S8. The energy spectrum of the Ag_2O/rGO hybrid aerogel after co-capturing Cs^+ and I^-.

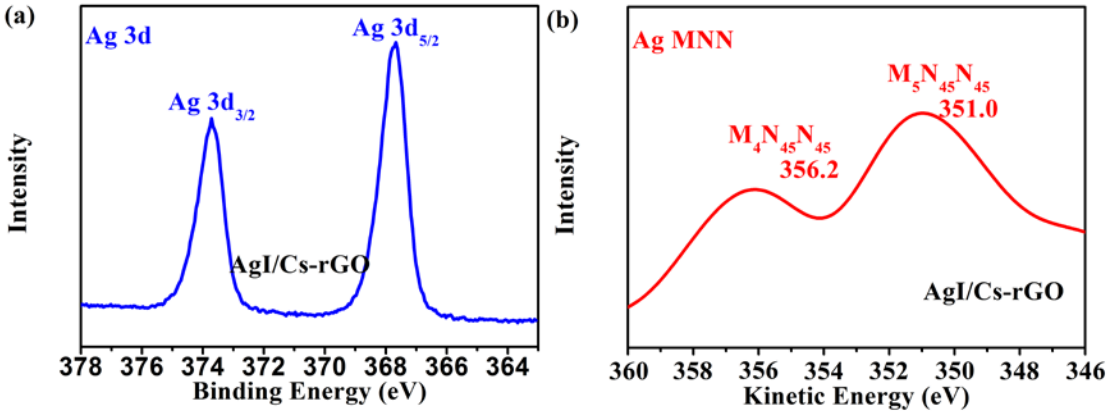

Figure S9. XPS spectra of the Ag_2O/rGO hybrid aerogel after light irradiating.

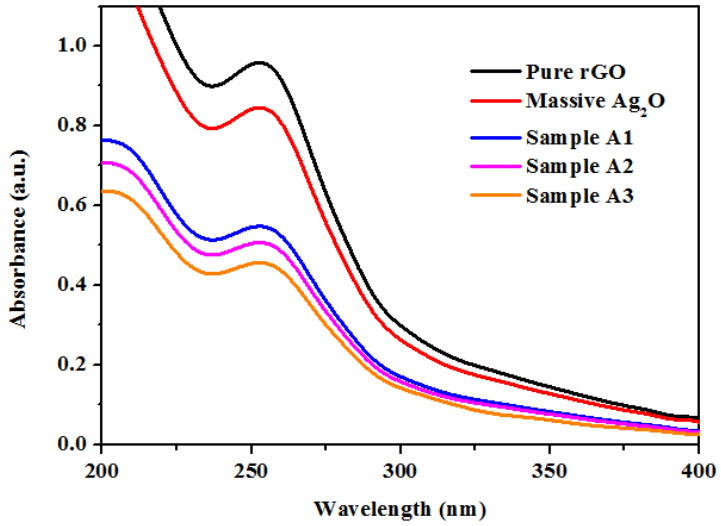

Figure S10. NBT transformation absorbance spectra over pure rGO, massive Ag_2O, and sample A1-3 for 4 h, respectively.

Table S1. The specific surface areas and pore size distribution of those samples.

Samples	S_{BET} (cm^3 g^{-1})	Pore volume (cm^{-3} g^{-1})
Massive Ag_2O	26.3	0.11
Sample 3	665.4	0.39
Sample 2	601.7	0.28
Sample 1	514.8	0.64

Table S2. The relevant element compound of those samples.

Samples	Atomic % (C)	Atomic % (Ag)	Atomic % (N)	Atomic % (O)	Mass ratio of Ag_2O to rGO
rGO	77.49	-	7.52	14.99	-
Sample 3	71.89	1.47	3.09	23.55	0.104
Sample 2	71.09	3.18	3.17	22.56	0.297
Sample 1	70.19	4.75	2.97	22.09	0.457

Table S3. The adsorption capacities in comparison with previous work.

Adsorbents	Adsorption Element	Removal Capacity (mmol/g)	Reference
K-Merlinoite	Sr^{2+}	0.50	Ref. 35
	Cs^{+}	0.75	
MWCNT reinforced Zeolite-A beads	Sr^{2+}	1.22	Ref. 36
	Cs^{+}	0.85	
Titanate nanofibers	Cs^{+}	0.55	Ref. 23
	I^{-}	3.04	
Titanate nanofibers	Sr^{2+}	0.63	Ref. 37
Layered Double Hydroxides	I^{-}	3.72	Ref.38
Anion-exchange membranes	Br^{-}	0.438	Ref. 39
Chitosan-based anionic exchanger	Br^{-}	0.72	Ref. 40
δ-Bi_2O_3 aerogels	I^{-}	2.04	Ref. 7
Ag_2O/rGO aerogel	Sr^{2+}	1.75	This work
	Cs^{+}	0.86	
	Br^{-}	5.24	
	I^{-}	4.32	